Comments on Modern Physics, 2:A261–A283, 2002

1560-5892/02 $12.00 + .00

THE AUGER OBSERVATORY AND PHYSICS OF THE HIGHEST ENERGY COSMIC RAYS

PAUL SOMMERS

High Energy Astrophysics Institute, University of Utah Physics Department, Salt Lake City, Utah, USA

Physicists from 54 institutions in 19 countries are working together to construct the Pierre Auger Cosmic Ray Observatory. This project is committed to studying the sources of the highest energy cosmic rays. The surprising accumulation of evidence that the high end of the energy spectrum is *not* strongly affected by the cosmic microwave background radiation defies any mundane explanation. Theories for this necessarily entail some novel astrophysical hypotheses or physics beyond the standard model. To resolve these issues, the Auger Observatory is designed to have enormous collecting power with exposure to the entire sky. High quality "hybrid" air shower measurments utilize data from a surface array of particle detectors in conjunction with data from atmospheric fluorescence detectors.

1. INTRODUCTION

Accounting for surprising cosmic ray observations has been a challenge to physicists ever since the first measurements by Victor Hess in 1912. Today's observations pose the toughest puzzles ever. It was in 1938 that Pierre Auger discovered the occurrence of air showers produced by cosmic rays, and he correctly inferred that Nature somehow produces particles with energies up to at least 10^{15} eV. Subsequent experiments have found evidence for still higher particle energies. In 1962, Volcano Ranch recorded an air shower whose primary particle apparently had an energy greater than 10^{20} eV [1]. The discovery of cosmic microwave radiation came several years later, and Greisen [2] and Zatsepin and Kuzmin [3] (GZK)

Received 14 April 2001; in final form 23 May 2001.

I am grateful to Carlos Escobar for encouraging me to write this and to Roger Clay and Brian Fick for stimulating conversations during its preparation. Brian Fick also supplied the figure showing the engineering configuration. I thank Ken Simpson for the AIRES/Sibyll simulation results used in Figure 2.

Address correspondence to Paul Sommers, High Energy Astrophysics Institute, University of Utah Physics Department, 115 S. 1400 E, Room 201, Salt Lake City, UT 84112-0830. E-mail: sommers@physics.utah.edu

then pointed out that the universe should be almost opaque to such high energy cosmic rays. (In the rest frame of such an energetic nucleon, the microwave photons are a beam of gamma rays with energies exceeding the pion restmass. The production of each pion typically takes about 20% of the nucleon's energy as measured in the universal restframe [4].) It has therefore been surprising to see the accumulation of evidence that the cosmic ray spectrum continues unabated above the expected GZK cutoff. (See the review article by Nagano and Watson [5] for current details about the observational evidence.)

It is challenging just to explain how Nature can accelerate particles to such phenomenal energies. A satisfactory understanding of the highest energy cosmic rays must also explain why there is no GZK spectral cutoff and why the observed super-GZK particles do not have arrival directions correlated with interesting astrophysical objects [6, 7]. In fact, there is no evident anisotropy in the arrival directions of cosmic rays above the spectrum's ankle. The magnetic rigidity of the super-GZK particles is so high that their trajectories should be only slightly deflected by known magnetic fields within the Galaxy or by extragalactic fields within the GZK distance limit. The fact that the arrival directions do not correlate with galactic structure or with powerful extragalactic sources within the GZK distance limit constitutes a profound puzzle.

There is already a large body of literature pertaining to the problem of explaining these observations. Some recent reviews are by Cronin [8], Olinto [9], Nagano and Watson [5], and Sigl [10]. The cursory discussion here is only meant to highlight the need for a full-sky observatory with enormous exposure and high quality measurements.

It is the continuation of the energy spectrum beyond the expected GZK cutoff that makes it hard to account for the observations. Without the super-GZK particles, the problem would be to determine which of many source models is correct (radio galaxy hot spots, gamma-ray-burst fireballs, etc.). The absence of a cutoff has proved difficult to explain without new physics, and this places a heavy burden of proof on the observational side. Measurements of the energy spectrum above the GZK threshold are eagerly awaited from stereoscopic HiRes [11] and the Japanese Telescope Array [12, 13] as well as from the Auger Observatory.

Sources of high energy cosmic rays have almost certainly been active in the universe for billions of years. At energies below the GZK threshold, cosmic rays suffer very little attenuation due to nuclear collisions, $e^{\pm}$ pair

production, synchrotron radiation, pion photoproduction in collisions with infrared or visible photons, or by any other known mechanism. The universal population of sub-GZK particles should therefore have a mean age that is measured in billions of years. Above the GZK threshold, however, particle energies are attenuated in less than 100 million years. This large difference in accumulation times means there is necessarily a big spectral drop at the GZK threshold in any universal population of high energy cosmic rays. The most common way to explain the *absence* of that drop in the observed spectrum is by invoking some model in which the observed sub-GZK particles also have a mean age less than 100 million years.

Sub-GZK particles that are detected on Earth would be sufficiently young if the sources are in the Galaxy or its halo. High energy cosmic rays escape rapidly from the Galaxy. The fact that arrival directions do not favor the galactic center or the galactic disk is powerful evidence that the sources of these high-rigidity particles (above the spectrum's ankle, say) are not congregated in the disk. Sources distributed in a large halo, however, could produce a distribution of arrival directions that is isotropic enough to be consistent with the observations made so far. The only candidate galactic accelerators to such high energies are associated with collapsed stars. There is no stellar distribution of large enough extent to produce the required cosmic ray source distribution, however. Theories of halo production of cosmic rays have therefore invoked new physics in which the decay of massive relic particles produces the highest energy cosmic rays without acceleration [14, 15, 16], or else energetic neutrinos from distant AGNs interact with a halo of low-energy relic neutrinos [17]. Regardless of how the particles are produced, a halo distribution of sources should cause a dipole anisotropy, since we are at least 8 kpc from the center of the distribution. The full-sky Auger Observatory is designed to detect such non-uniformity in arrival directions [18]. The sub-GZK particles provide rich statistics for this. Composition analysis can also test this model of decaying massive particles. Decays of relic particles should yield nucleons and gamma rays, but detection of any nuclei would rule out such models. The Auger Observatory has two complementary types of detectors in order to obtain maximum information about the primary particle mass distribution.

The approximate isotropy of observed arrival directions might not exclude sources in the galactic disk if the particles are highly charged

nuclei. Neutron stars could perhaps accelerate iron nuclei to the highest observed energies [19, 20, 21]. The Fly's Eye and HiRes/MIA data favor a light mass composition above the ankle [22, 23], but there is some uncertainty in the interpretation of AGASA composition data [24]. More definitive composition and anisotropy results are needed to decide whether or not a picture of heavy nuclei originating in the galactic disk is clearly excluded.

A young sub-GZK population is hard to explain if the sources are extragalactic. One needs a local overdensity of sources in a region from which the sub-GZK particles can escape in less than 100 million years. The local cosmic ray luminosity must be nearly two orders of magnitude greater than the universal average, since cosmic rays from the local sources are allowed to accumulate for less than one tenth as long, and the local cosmic ray density must dominate the universal density in order to mask the GZK suppression that has to exist in the universal population. Neither the Local Group of galaxies nor the larger Virgo supercluster provides us with such a large matter overdensity (the overdensity being only a factor of 2 or 3 for those cases). An extragalactic model without a GZK suppression requires some small leaky volume around us which is remarkably productive in high energy cosmic rays.

It is possible that Cen A was recently a strong source of high energy cosmic rays [6, 25]. At a distance of only 3 Mpc [26], it could explain a large density of young cosmic rays above and below the GZK threshold. It has the large double-lobe structure characteristic of the most luminous radio galaxies like Cygnus A, although the radio luminosity of Cygnus A is presently 1,000 times stronger than that of Cen A. If that luminosity difference is due to the Cen A engine turning off (e.g. the very strong radio flux at Earth may have ended 10 million years ago), then we would not expect to see cosmic rays coming directly from that direction today even though intergalactic magnetic fields might have turned around enough of the high energy cosmic rays for them to dominate our observed spectrum. Intergalactic fields of sufficient strength to do this may be plausible [6, 25] but those strong fields are not known to exist and need to be verified. If we had been watching 10 or 20 million years ago we might have seen a brilliant cosmic ray source in the southern sky, wheraes today we may be bathed in its diffuse afterglow. This Cen A explanation is anti-Copernican in the sense that we are in a special place and time where we can observe super-GZK particles that are highly suppressed

in generic parts of the universe. An anti-Copernican explanation is hard to avoid, however, without invoking new physics to account for the unabated super-GZK spectrum. Cen A has long been considered to be a candidate source [27], and detailed analyses support the view that radio galaxy hot spots could accelerate protons to super-GZK energies [28]. A population centered on Cen A would induce a dipole anisotropy at Earth in sub-GZK as well as super-GZK particles. The full-sky Auger observatory will have the sensitivity needed to investigate this hypothesis that Cen A is the dominant source of observed high energy cosmic rays.

Not all explanations for the absence of a GZK cutoff rely on young particles below the GZK threshold, but the alternatives are exotic in the sense of invoking non-standard physics. Some look for ways that all the high energy particles can be *old*. This requires super-GZK particles that are immune to degradation by the background radiation (e.g. stable supersymmetric neutral hadrons [29] or neutrinos), or it can be done by a violation of the Lorentz invariance [30, 31] that is used to derive the GZK suppression.

With a sufficiently hard source spectrum, it may be possible to account for the observed spectrum with old sub-GZK particles and young super-GZK particles, i.e. the ages that are normally expected. Top-down theories (e.g. topological defect annihilation [32]) predict the production of so many super-GZK particles that they would be observable despite their having accumulated for a relatively short amount of time compared to the sub-GZK population. Just above the threshold, one expects a dip or apparent "gap" in the energy spectrum in these models. This spectral feature can be checked along with the expectations in this model that there should be strong gamma ray and neutrino components with no ($A > 1$) nuclei.

The high energy cosmic ray observations are even more puzzling if one considers the evidence for tight clusters of arrival directions seen in the AGASA data [33]. The direction coincidences are within experimental resolution, even for events that differ in energy by a factor of 2 or more. If these clusters are not a statistical anomaly, then it suggests that the primary particles are neutral or the sources are very close to us. Looking for such clusters has to be a high priority for Auger and other experiments.

There is no mundane way to account for the present observational results. Some unexpected astrophysics or physics beyond the standard model is part of any explanation. Still, there is no shortage of suggestions. Theories are like the heads of the mythological Hydra: whenever one

is cut off by new observational constraints, others appear to take its place. Rather than simply testing the consistency of different hypotheses, we need to make a positive identification of the sources. The spectrum and composition measurements can be effective in excluding classes of theories, but they are unlikely to lead to a signature that picks out one specific model. Full-sky detailed anisotropy analysis is the best hope for positively identifying the origins of the high energy cosmic rays.

The Auger Observatory has been designed to be sensitive to the entire population of cosmic rays above the spectrum's ankle with full efficiency above 10^{19} eV. All of these particles presumably have a common source type. The rich statistics of the sub-GZK population may provide the best fingerprint for identifying the sources. Standard physics explanations for the absence of the GZK suppression involve some reason for the sub-GZK particle population to be as young as the super-GZK population. In that case, all of the Auger particles must originate in relatively nearby sources, and a careful analysis of their arrival directions should identify those sources.

2. THE PIERRE AUGER OBSERVATORY

Jim Cronin visited Alan Watson and the site of the Haverah Park detector in 1991. By early 1992, the idea for a giant array to study the highest energy cosmic rays was germinating. Cronin circulated a "Design Concept" memo [34] early in that year, and an international workshop was held in Paris in April, 1992 [35]. A series of other workshops culminated in a six-month design study at Fermilab in 1995 and production of the Pierre Auger Project Design Report [36]. Primary tenets of the design are these:

- Full-sky exposure by having installations in both the southern and northern hemispheres.
- Enormous collecting power by virtue of an array area of 3000 km^2 in each hemisphere.
- Hybrid measurements using both the surface array of water Cherenkov detectors and atmospheric fluorescence detectors.

An international collaboration of physicists from 19 countries formed, and the Mendoza (Argentina) site for the southern installation was chosen at the collaboration meeting in Paris in 1995. A year later, a site for the northern hemisphere was selected in Utah (USA). Financial commitments have been

secured from science funding agencies in the participating countries, and ground breaking occurred for the southern site in March, 1999. A two-year engineering phase is culminating this year, and full construction is expected over the next few years.

The Auger Collaboration includes physicists in Argentina, Armenia, Australia, Bolivia, Brazil, China, the Czech Republic, France, Germany, Greece, Italy, Japan, Mexico, Poland, Russia, Slovenia, the United Kingdom, the United States, and Vietnam.

The engineering phase of the project consists of 40 Cherenkov water tanks deployed in a hexagonal array east of Malargue in Mendoza Province. Each water tank has a circular area of 10 m^2 and 1.2-meter height, with 3 large phototubes recording light pulses with flash ADC electronics. Solar panels provide power for the electronics and radio communications. There are no cables to the surface detectors. The air above the engineering surface array is observed at night by two Schmidt-optics prototype fluorescence telescopes, each having an aperture diameter of 2.2 meters and a $30° \times 30°$ field of view. See Figure 1 for the configuration of the hybrid engineering array.

When completed, each hemisphere's installation will cover an area of 3000 km^2, instrumented with approximately 1600 water tank detectors. Each tank has 6 nearest neighbors separated by 1.5 km. There will be fluorescence "eyes" with multiple telescopes for measuring the UV light from atmospheric nitrogen fluorescence above the array. For the southern site, there will be three eyes on the perimeter looking only inward and one eye at the center with 360° azimuthal coverage. Data from the water tank detectors will be concentrated by communication towers at each eye and conveyed by microwave links to the central data acquisition system.

With 6000 km^2 total area and full acceptance out to 60° in zenith angle, the Auger full-time acceptance is 14,000 $km^2 \cdot sr$. The intensity of cosmic rays above 10^{19} eV is known to be about $.5/(km^2 \cdot sr \cdot yr)$, so the Auger Observatory should measure 7000 cosmic rays per year above 10^{19} eV. If the energy spectrum is a simple power law with differential index 2.7, then 140 per year above 10^{20} eV are expected.

Jim Cronin and Alan Watson are the spokespersons for the project. The project management is hosted by Fermilab. Detailed technical information is readily available on the World Wide Web. Most of the collaborating institutions have web sites. The URL www.auger.org is the primary site and includes the archive of technical papers known as "GAP notes" (a name held over from the original "Giant Array Project" designation).

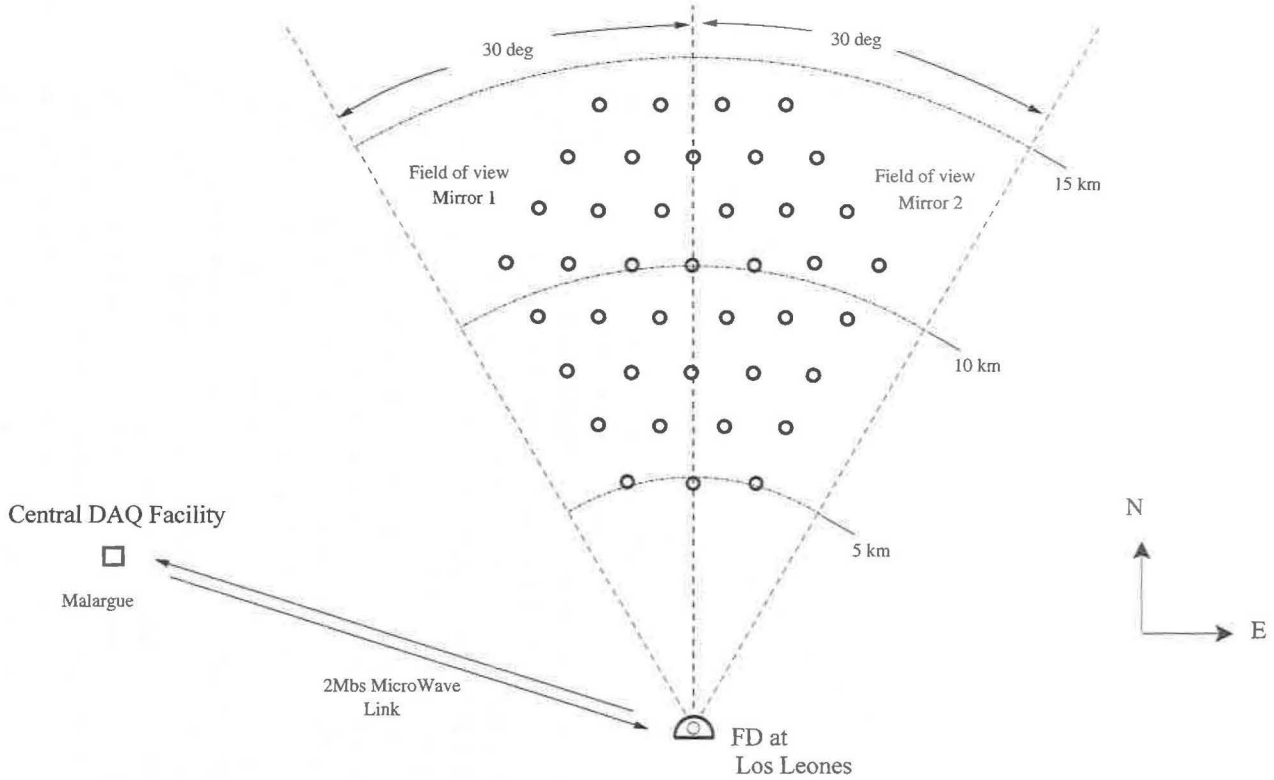

FIGURE 1. Map of the engineering array showing the location of 40 water Cherenkov tanks beneath the aperture of two fluorescence detector prototype telescopes.

The following sections of this paper discuss why the Auger Observatory has been designed with a full-time surface array along with fluorescence detectors for measuring air showers in the atmosphere on clear nights. Approximately 90% of the Auger showers are expected to have measurements at ground level only. Arrival times of the shower front at different water tanks will determine the arrival direction of the primary cosmic ray. Its energy is obtained from the particle density at one kilometer from the shower core. The atmospheric depth of the chosen sites is such that the high energy air showers at typical zenith angles reach their maximum particle densities at approximately that slant depth for densities measured 1 km from the core. Because a smooth function is stationary at its maximum, shower density measured at 1 km from the core is little affected by fluctuations in shower development, and zenith angle corrections are minimal. Composition is studied via shower muon content in the water tanks. With high particle densities, a rapid signal rise can be used to infer a strong muon contribution, and for the low particle densities far from the core, individual muon Cherenkov pulses can be counted.

When the fluorescence detector (FD) is operating (at least 10% of the time), the shower size will also be measured as a function of depth in the atmosphere, giving the "longitudinal profile" of the shower. Geometric reconstruction of the shower axis (direction and core position) is well determined by the FD pixel signal strengths and the combined *timing* information from the FD pixels and the surface detectors [37, 38]. (Note that the shower axis is determined in hybrid mode without using relative amplitudes of the surface detectors, so the particle densities are measured at core distances that are known without reference to the density measurements.) The integral of the longitudinal profile measures the total energy in the electromagnetic cascade, which is approximately 90% of the primary particle's energy. The atmospheric depth X_{max} where the shower reaches maximum size is statistically anti-correlated with the primary particle's mass, so the FD measurements of X_{max} give an important additional handle on the mass composition. The relatively small hybrid data set will have excellent energy resolution and the best possible composition data. It will be of great value in its own right, and reconciling the surface-only reconstructions with the hybrid reconstructions in the hybrid data set will correct any systematic errors that may initially exist in the surface-only shower reconstruction algorithms.

The FD and SD (surface detector) are complementary in some important respects. The SD has an unambiguous time-independent aperture. Its

operation is continuous and automatic, and through-going muons provide a reliable calibration tool for the water Cherenkov detectors. A potential criticism is that some modelling of hadronic interactions and shower development is used to relate particle density measurements to shower energy and primary mass likelihood. The longitudinal profile measured by the FD provides a nearly model-independent energy determination for each shower, and the distribution of X_{max} values is a powerful indicator of the primary mass composition. However, its operation (requiring darkness and good weather) is more complicated, there is not an automatic way to do absolute calibration of the telescopes, and the atmosphere must be monitored carefully in order to fulfill its potential. Errors in modeling atmospheric absorption of fluorescence light and scattering of the air shower's Cherenkov light can lead to errors in the longitudinal profile. The surface density and vertical distribution of aerosol particles (including clouds) both change with time, and at any one time they may vary over the large spatial aperture of the observatory. The SD is simple and robust, but some model dependence enters the data analysis; the FD relies less on interaction models, but its sensitivity is time-dependent and it requires diligent monitoring. The combination can overcome weakneses in both techniques.

3. MAPPING THE COSMIC RAY SKY

There is great advantage in a cosmic ray observatory having exposure to the entire celestial sphere, especially if the relative exposure is nearly uniform. In that case, scatter plots of arrival directions are immediately interpretable, and eyeball evaluations can readily identify discrete sources or large-scale patterns. Discrete sources will be identified with equal sensitivity anywhere in the sky. If no such sources are found, the flux upper limits will be uniform over the sky.

Full-sky coverage is crucial for large-scale anisotropy analysis. It makes it possible to do integrals over the sky, so the powerful tools of multipole moments and angular power spectra are available. With full sky coverage, cosmic ray anisotropy analysis will be similar to gamma ray burst anisotropy analysis. The numbers of events will be comparable, the direction error boxes will be comparable, the exposure non-uniformities will be comparable, and in both cases events come from all parts of the sky. All of the techniques that were employed to search for anisotropy in the

BATSE data [39, 40] can be applied to a full-sky cosmic ray data set. Any cosmic ray deviations from isotropy will be of immediate interest, since there is presently no proven anisotropy at the highest energies. Unlike the COBE anisotropy analysis, for example, it will not be necessary to subtract a large known dipole pattern and a myriad of uninteresting foreground sources.

The role of an observatory is to map the sky and make the results available to the scientific community. This is highly challenging for an observatory without full-sky coverage. Measurements in that case are made with different sensitivity in different parts of the sky, and nothing at all can be said about a large hole where the exposure is zero. Certainly it is not possible to perform the full-sky integrations that are required to measure the multipoles of the celestial cosmic ray intensity.

The Auger Observatory will map the sky and make results available in a form which is readily usable without special knowledge of the detector properties and which is independent of any theoretical hypothesis. Low-order multipole tensors (or spherical harmonic coefficients) summarize the large-scale information. The angular power spectrum reveals if there is clumpiness on smaller scales. These anisotropy results will be tabulated so that theorists can test arbitrary models quantitatively without privileged access to the data. The spherical harmonic coefficients are computed using weight factors that compensate for the observatory's small exposure non-uniformity in declination [18].

While the role of an observatory should be to map the sky and determine the patterns without preconceived expectations, it is nevertheless worthwhile to consider what might be learned by measuring the low order multipoles.

There is no information about anisotropy patterns in the *monopole* scalar by itself. It is simply the sky integral of the cosmic ray intensity. That is information already present in the energy spectrum. A pure monopole intensity distribution is equivalent to isotropy. The strength of other multipoles relative to the monopole is a measure of anisotropy.

A predominantly dipole deviation from isotropy might be expected if the sources are distributed in a halo around our Galaxy [14, 15, 16]. In this case, one expects the dipole vector to point toward the galactic center. An approximate dipole deviation from isotropy could also be caused by a single strong source (e.g. Cen A) if magnetic diffusion or dispersion distributes those arrival directions over much of the sky. In general, a single source would produce higher-order moments as well.

A dipole deviation from anisotropy may be associated with any cosmic ray density gradient. If the magnetic field is disorganized, the gradient produces streaming by diffusion and the dipole vector is parallel to the density gradient. If there is a regular magnetic field, however, the expected dipole vector $\vec{D}$ can be perpendicular to both the gradient and the field direction, $\vec{D} \propto \vec{\nabla}\rho \times \vec{B}$. The direction of strongest intensity corresponds to the arrival direction of particles whose orbit centers are located in the direction of increased density.

An equatorial excess in galactic coordinates or supergalactic coordinates would show up as a prominent *quadrupole* moment. A measurable quadrupole is expected in many scenarios of cosmic ray origins, and is perhaps to be regarded as a likely result of a sensitive anisotropy search. (Evidence for a supergalactic equatorial enhancement has been cited [41, 33] but not confirmed [42].) The axis of a symmetric quadrupole distribution might differ from the galactic axis or the supergalactic axis if we are embedded in a magnetic field that systematically rotates the arrival directions.

The precision in determining multipole moments depends on the number of arrival directions as well as the uniformity of exposure. The Auger sensitivity has been evaluated quantitatively as a function of the number of arrival directions [18]. Given the Auger aperture, the number of arrival directions depends simply on the energy cut and length of running time.

4. THE ENERGY SPECTRUM IN DETAIL

Independent of any anisotropy that may or may not be observed, the energy spectrum of cosmic rays can provide important information about their sources and their propagation [43]. The details of the energy spectrum may depend on properties of the population of sources (e.g. the distribution of maximum rigidity of produced particles and magnetic confinement at the sources). It also is affected by the GZK suppression and therefore is sensitive to the distribution of source distances. The spectrum predicted for the topological defect annihilation scenario is markedly different from predictions based on accelerative mechanisms. The topological defect scenario predicts a spectral dip or "gap" due to the GZK effects, and the gap's structure can depend on the spatial distribution and past evolution of the topological defects.

Accurate and verifiable measurements of air shower energies are essential for extracting specific information about the nature of cosmic ray sources from detailed structure in the energy spectrum.

If it turns out that there are observable discrete sources, then much can be learned by studying the showers coming from those particular directions. The source's energy spectrum is of special interest for understanding the astrophysical processes which account for the high energy cosmic rays. Also, by correlating energies with magnetic deflections from a known source, it is possible to learn about the intervening magnetic fields, both galactic and extragalactic. Accurate energy measurements are crucial for this.

A major function of the Auger fluorescence detectors is to provide accurate energy measurements without reference to any specific hadronic interaction model. A reliable measurement of a shower's longitudinal profile gives an unambiguous measurement of the energy in its electromagnetic cascade. This is a firm lower limit for the cosmic ray's energy and it leads to the best estimate for the actual energy.

Hadronic interaction models extrapolated from energies probed with laboratory colliders predict that approximately 90% of of the primary's energy is dissipated by the electromagnetic cascade resulting from neutral pion decays. The remaining energy is in the form of muons and neutrinos, primarily from charged pion decays. There is some dependence on the primary particle's mass. A proton shower typically dissipates about 95% of its energy in the electromagnetic cascade whereas the fraction for an average iron shower is closer to 85%. By assuming that the electromagnetic shower energy represents 90% of the total, the systematic error should not be greater than 5%, regardless of what the mass distribution may be. The error on any individual shower energy can be greater than this because of fluctuations in the fraction of energy taken by muons and neutrinos, but if the shower energy is assumed to be 1/0.9 times the electromagnetic energy, then the *systematic* error due to the unknown composition should not exceed 5%.

Those hadronic models are not unquestionably correct, since they have not been tested experimentally. It is possible to devise consistent models in which a large amount of the primary energy is frequently given to prompt muons or other particles that do not contribute to the electromagnetic cascade. In that case, shower energies derived from measurements of the electromagnetic cascade could be systematically too low. There is no

evidence supporting any such hypothesis, however. It should also be noted that such a model would imply that the mysterious super-GZK particles might be even farther beyond the expected spectral cutoff than has been claimed.

The surface array also has good capability for measuring shower energies, and the two components of the hybrid detector serve as cross checks on each other. The surface array is limited to measuring the cascade at just one atmospheric depth, so the calorimetric method of the fluorescence detector is not applicable, and an error in the hadronic model could cause systematic error in shower energies. As discussed in the next section, the hybrid data set should provide empirical algorithms that eliminate systematic error, so the entire data set from the surface array can be used for a high-statistics energy spectrum determination.

The surface array will also play an important role in the hybrid spectrum determination by giving an easy-to-compute aperture. The energy of each shower detected by the surface array while the fluorescence detector is operating should have a high quality fluorescence-assisted energy determination. To convert the energy distribution to a spectrum, one also needs to know the aperture accurately as a function of energy. Atmospheric variation can make that difficult to calculate for a fluorescence detector alone. For a hybrid detector, however, the exposure can be computed simply as the product of the surface detector acceptance and fluorescence detector run time.

The surface array and fluorescence detector work symbiotically in measuring shower energies in hybrid mode. Each gives an estimate for the shower size at the surface, and the two estimates serve as cross checks when both are well measured. For some showers measured at long range by the fluorescence detector, the surface array's estimate of shower size provides a valuable way to check the atmospheric attenuation. If the attenuation uncertainty is large for distant events on some nights, the surface array's size determination offers a way to normalize the longitudinal profile.

The fluorescence detector in combination with the surface array provides high resolution measurements down to about 10^{18} eV. Although the aperture is smaller than at 10^{19} eV, there will be ample statistics due to the higher cosmic ray intensity. Detailed simulations show that the detector will make quality shower measurements in hybrid mode for all energies greater than 10^{18} eV [38].

5. THE PRIMARY PARTICLE TYPES

The surface array is the cost-effective way to get the high statistics and uniform exposure needed for a sensitive anisotropy analysis, and the fluorescence detector provides reliable energy measurements for the energy spectrum. When it comes to determining the cosmic ray mass composition, however, the combination of the two detector components is especially fruitful. The hybrid data set will have high sensitivity to the primary masses.

Knowing the particle types is essential for an understanding of the high energy cosmic ray sources. If there are nuclei other than protons, for example, then the top-down scenarios involving massive particle decays can be excluded. The presence of heavy nuclei would also constrain the photon environment of any astrophysical accelerator since high energy nuclei would photodisintegrate at the source if photon densities are high. Since energetic nuclei can also photodisintegrate while in transit as a result of collisions with cosmic microwave and infrared photons, the distribution of particle masses is a useful handle on the distribution of pathlengths from the sources. The study of the high energy composition should also include a search for photon and neutrino primary particles, as these are expected to be prominent if top-down processes are responsible for the highest energy cosmic rays. The Auger Observatory can recognize a neutrino flux by recording nearly-horizontal electromagnetic showers near the surface for which the primary particle must have interacted deep in the atmosphere [44].

If discrete sources are identified, then it will be important to study the composition of particles coming from each of them. The particle masses will say much about the astrophysical conditions and processes at the source. Since the arrival directions will also be used to probe intervening magnetic fields, it is important to know the rigidities of the detected cosmic rays. Measuring the energy is not enough; the charges of the particles must also be estimated. Since a nuclear charge is approximately half the nucleon number, it suffices to determine the masses of cosmic ray particles.

Given an accurate energy estimate, the muon content of a shower is a good indicator of the primary mass. Heavier nuclei produce showers with more muons. An iron shower produces, on average, 80% more muons than a proton shower of equal total energy. There is very little hadronic model dependence in this fact. It is largely due to the heavy nucleus shower

behaving as a superposition of subshowers from its individual nucleons. Relative muon numbers are therefore a model-independent effective handle on the primary mass. Figure 2 shows a scatter plot of muon number vs. depth of maximum (X_{max}) for showers of fixed energy. Iron and proton showers are indicated by different symbols. It can be seen that the muon number appears to be a better separator of the two components than is X_{max}.

In practice, experimental measurement fluctuations will limit the utility of muon measurements for primary mass determination. Instead of measuring the total muon number, the surface array will only sample the

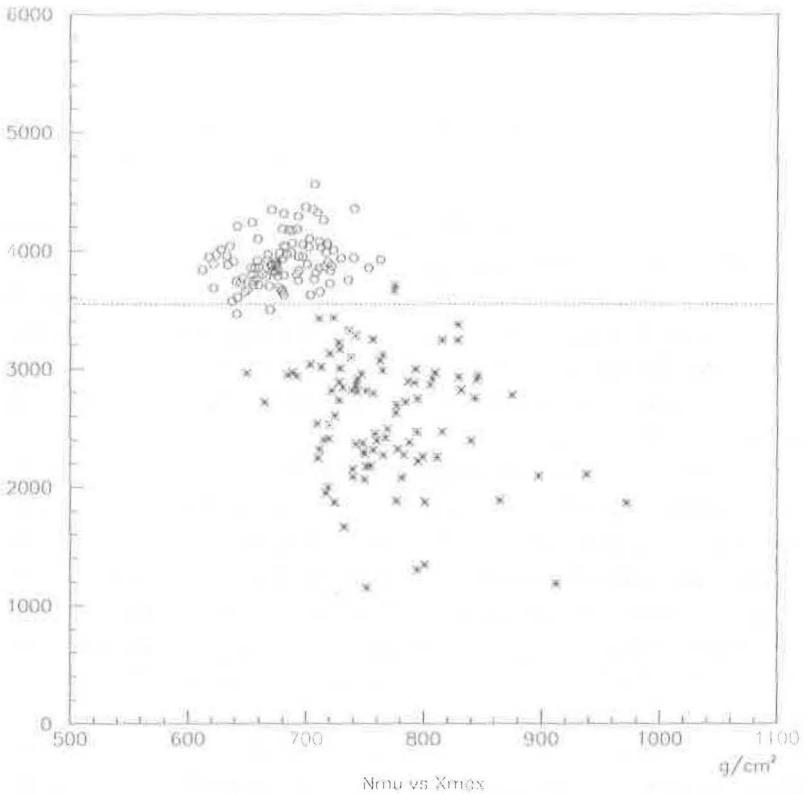

FIGURE 2. Muon number versus atmospheric depth of maximum X_{max} produced using AIRES/Sibyll simulation of 10^{19} eV showers. The detector is at altitude 1400 meters, and zenith angles are less than 30°. Open circles represent iron showers. The asterisks are proton showers.

density in 5 or more 10 m^2 water tanks, and muons can be individually counted only at large distances from the core. Even if muon identification is perfect, Poisson fluctuations in the numbers will introduce an important resolution limitation. (The muon density 1 km from the core is on the order of $1/m^2$ for 10^{19} eV showers. With 5 detectors triggering, the expected number is on the order of 50, and Poisson fluctuations should be roughly 15%. Imperfect muon identification will degrade this, but the fractional Poisson fluctuations decrease with increasing energy.) When coupled with experimental uncertainty in the shower energy, the uncertainty in muon density measurements may blur even the extreme mass components of iron and protons. Figure 3 shows what happens to the scatter plot of Figure 2 when the muon number is offset by an amount drawn from a Gaussian with $\sigma = 20\%$ and Xmax values are smeared by a 15-g/cm^2 Gaussian detector resolution function. The iron and proton distributions then overlap both in muon content and X_{max}. It is important to note, however, that the smeared distributions can be better separated by a diagonal line in that 2-dimensional scatter plot than they can be separated on the basis of either muons or X_{max} alone. In other words, the two handles, muons and X_{max}, provide a far better mass indicator in combination than does either one by itself. This indicates the strength of the hybrid detector for composition analysis.

It may be conceptually useful to think of the surface array as providing two measured quantities for each shower: ρ_{mu}, the muon density one km from the core, and ρ_{em}, the electromagnetic particle density 1 km from the core. Given any specific model (e.g. AIRES, CORSIKA, Sibyllized MOCCA, etc.), there is a mapping from shower energy and primary mass (E, A) to (ρ_{mu}, ρ_{em}). The map gives the expected values for the measured quantities, determined by many simulations of showers with fixed E and A. (The mapping also depends on zenith angle, but it can be determined separately for every zenith angle.) Figure 4 shows this mapping schematically. The inverse mapping is also well defined, and this is how the measured quantities are used to infer E and A. For any measured pair (ρ_{mu}, ρ_{em}), there is a unique energy and mass combination which gives that pair as the expected measured quantities. It is not required that the energy or mass be a simple function of the two measured quantities.

Energy and primary mass can be regarded as functions on the space of measured quantities. Curves of constant A, when mapped to (ρ_{mu}, ρ_{em}) space, tend to be diagonal lines in (ρ_{mu}, ρ_{em}) space. (Increasing E while

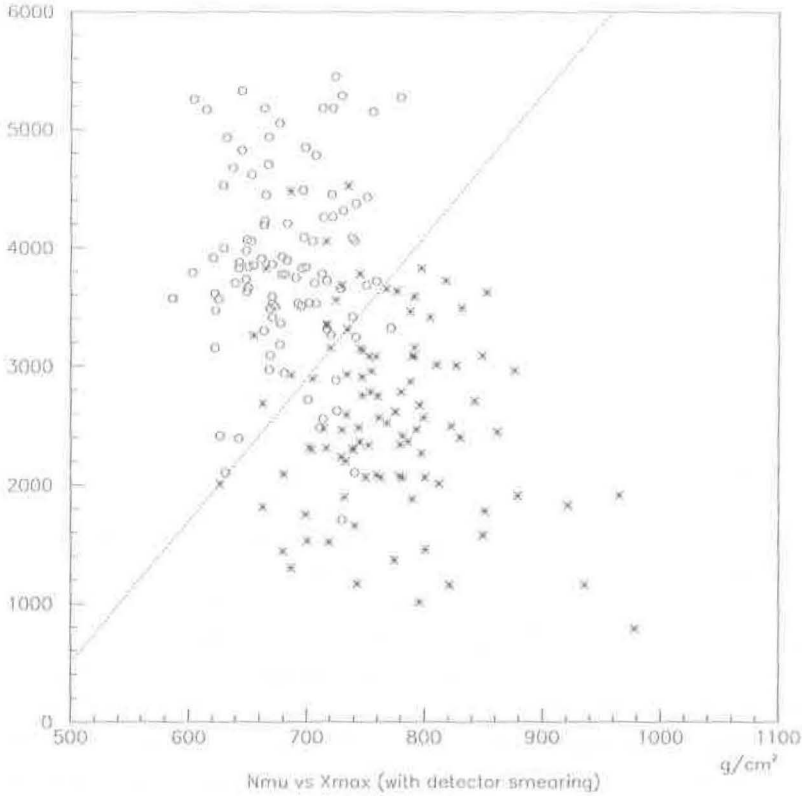

FIGURE 3. Here the muon number includes a detector uncertainty of 20%, and a detector resolution of 25 g/cm^2 has been applied to Xmax values. With this detector smearing, a diagonal line is needed for effective separation of iron from protons.

keeping A fixed tends to increase both ρ_{mu} and ρ_{em}.) The curves of constant E are diagonals transverse to the constant-A curves. (Increasing A while E is fixed tends to increase the muon content but decrease the electromagnetic particles since ground level would be further past the maximum of the more rapidly developed shower.)

Mapping all recorded showers to (E, A) space yields a 2-dimensional histogram. Fixing an interval of A-values then gives the energy distribution for that mass component; fixing an energy range gives the mass distribution at that energy.

Similarly, you can think of the fluorescence detector as providing two measured quantities: E_{em}, the electromagnetic cascade energy, and X_{max},

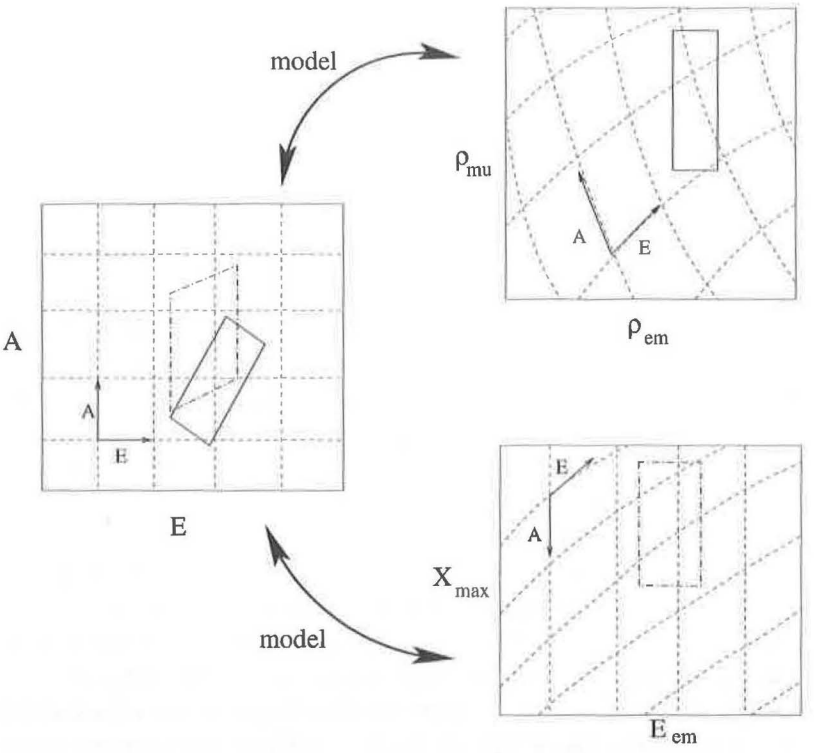

FIGURE 4. Shower simulations with a specific hadronic model give mappings from energy and mass (E, A) both to surface array quantities (ρ_{em}, ρ_{mu}) and to fluorescence detector quantities (E_{em}, X_{max}). A measured shower gives an error box in each space of measured quantities, and these can be mapped back to a pair of error boxes in (E, A) space.

the atmospheric depth of the cascade maximum. There is also a two-way mapping between this space and the (E, A) space. In this case, the curves of constant E are roughly parallel to the lines of constant E_{em}. The constant-A curves slope upward in X_{max} with increasing E in accordance with the elongation rate. It should be noted that the Fly's Eye data, in this picture, originally gave a 2-dimensional scatter plot which was unphysical inasmuch as it extended to A-values in excess of 56. This suggested that the hadronic interaction model used to map from (E_{em}, X_{max}) to (E, A) was unsatisfactory. The Gaisser-Stanev-Tilav minijet model (similar to Sibyll) was adopted to bring the scatter plot into the physically sensible region [45]. It has been argued [46] that any plausible model which is

physically acceptable in this sense will preserve the observed feature of the scatter plot points moving to lower A-values with increasing energy. Hence the Fly's Eye data have been used both to constrain the hadronic interaction models and make a statement about composition changing over the measured energy range.

The picture of Figure 4 provides a useful way to exhibit the advantage of a hybrid detector. A shower measured in hybrid mode gives a rectangular error box in both (ρ_{mu}, ρ_{em}) space and (E_{em}, X_{max}) space. Their images in (E, A) space should overlap, and the true energy E and mass A should be in the intersection region. If the error box images from the two methods are systematically incommensurate, then there is a clear indication of systematic measurement errors or, perhaps more likely, an inappropriate model for the mappings. Once the defects are corrected, the dual measurements will give invaluable cross checks, shower by shower. Together, they should restrict the allowed range of A for each shower more than either component could by itself.

The picture of Figure 4 also clarifies what it means to "train the surface array for energy determination." The fluorescence detector's E_{em} provides a reliable estimate for E. The hybrid data set is used to make sure that the mapping from (ρ_{mu}, ρ_{em}) space to (E, A) at least gets the energy right on average. The surface array by itself can then be trusted to determine the energy spectrum with the full data set. Even if the energy resolution is not as good as for the hybrid data set, at least the systematic errors should be eliminated. In a similar way, the hybrid data set may be able to validate (or adjust) the composition determination that is based on the larger data set of shower measurements by the surface array alone.

The analysis here has focused on just two measurable quantities for the surface array and the fluorescence detector. The analysis might also be able to take advantage of the signal rise time and a lateral distribution steepness parameter in the case of the surface array. With the fluorescence detector, one can try to measure also the longitudinal profile width (e.g. full width half maximum in g/cm^2) and the steepness of the profile's rising edge. These extra parameters may provide additional sensitivity to the primary mass when used in a multi-dimensional analysis.

Much careful work has been done in analyzing the capability of the Auger surface array on its own to measure shower energies and primary masses. Results can be found in the Design Report [36] and Auger technical notes [47].

6. SUMMARY

Cosmic ray observations at the highest energies constitute a puzzle that defies any conventional explanation. Understanding the origins of these particles will yield new astrophysical insights or physics beyond the standard model. The international Auger Project has organized itself to make a comprehensive study of cosmic rays above the ankle of the spectrum so as to unravel the mysteries of their production and propagation.

The Auger Observatory is a hybrid detector consisting of a giant surface array together with a fluorescence detector of matching aperture. Its design is based in part on the following important considerations:

- A continuously operating surface array provides uniform exposure in right ascension and time-invariant declination acceptance. It is the cost-effective way to get the enormous exposure that is needed to resolve the mysteries of the highest energy cosmic rays.
- Full-sky coverage with nearly uniform celestial exposure alllows accurate measurements of the multipole moments that are the best way to summarize and report large-scale anisotropy patterns. The large exposure and full-sky coverage also optimizes the search for discrete sources.
- The fluorescence detector makes a calorimetric measurement of the electromagnetic shower energy. This is a model-independent lower bound for each cosmic ray's energy and can be scaled to obtain the best estimate for the particle's total energy. The hybrid exposure is fixed by the surface array's invariant aperture and the fluorescence detector's run time. The hybrid data set therefore yields an unambiguous energy spectrum.
- Measurements of both X_{max} and muon density for a shower of known energy give two handles on the primary mass which, together, are more powerful than either by itself. The hybrid data set is therefore the basis for a sensitive determination of the cosmic ray particle types.
- Hybrid shower measurements enable valuable cross checks between the surface array and fluorescence methods. There is a history of dispute and skepticism between advocates of the different methods. The hybrid detector offers the only sure way to resolve those differences and gain the confidence of the entire community. Moreover, without both

components, it would be impossible to compare in detail the Auger results with those from all the other cosmic ray experiments.

- By comparing surface array measurements with fluorescence detector measurements shower-by-shower in hybrid mode, the analysis techniques for the surface array by itself can be tuned so that showers measured without the fluorescence detector can be used for a high-statistics determination of the energy spectrum and composition.

References

[1] J. Linsley, Phys. Rev. Lett. **10**, 146 (1963).
[2] K. Greisen, Phys. Rev. Lett. **16**, 748 (1966).
[3] G. T. Zatsepin and V. A. Kuzmin, Pis'ma Zh. Eksp. Teor. Fiz. **4** 114 (1966); [JETP Lett. **4**, 78 (1966)].
[4] C. T. Hill and D. N. Schramm, Phys. Rev. **D31**, 564, 1985.
[5] M. Nagano and A. A. Watson, Rev. Mod. Phys. **72**, 689 (2000).
[6] J. W. Elbert and P. Sommers, Ap. J. **441**, 151 (1995).
[7] N. Hayashida et al., Phys. Rev. Lett. **73**, 3491 (1994).
[8] J. W. Cronin, Rev. Mod. Phys. **71** S165 (1999).
[9] A. V. Olinto, Phys. Rep. **333-334**, 229 (2000).
[10] G. Sigl, Science **291**, 73 (2001).
[11] C.H. Jui, *AIP Conference Proceedings* **516** (26th Int. Cosmic Ray Conf. highlight paper) ed. B. L. Dingus et al. (1999).
[12] M. Teshima et al., Nucl. Phys. B (Proc. Suppl) **28B**, 169 (1992).
[13] The Telescope Array Design Report is available at www-ta.icrr.u-tokyo.ac.jp
[14] V. Berezinsky, M. Kachelriesz, and A. Vilenkin, Phys. Rev. Lett. **79**, 4302 (1997).
[15] M. Birkel and S. Sarkar, Astroparticle Physics **9**, 297 (1998).
[16] A. M. Hillas, Nature **395**, 15 (1998).
[17] S. Yoshida, G. Sigl, and S. Lee, Phys. Rev. Lett. **81**, 5505 (1998).
[18] P. Sommers, Astropart. Phys. **14**, 271 (2001).
[19] A. M. Hillas, Ann. Rev. Astron. Astrophys. **22**, 425 (1984).
[20] A. R. Bell, Mon. Not. R. Astron. Soc. **257**, 492 (1992).
[21] P. Blasi, R. I. Epstein, and A. V. Olinto, astro-ph/9912240 (1999).
[22] D. J. Bird et al., Phys. Rev. Lett. **71**, 3401 (1993).
[23] T. Abu-Zayyad et al., Phys. Rev. Lett. **84**, 4276 (2000).
[24] M. Nagano et al., Astropart. Phys. **13**, 277 (2000).
[25] G. R. Farrar and T. Piran, Phys. Rev. Lett. **84**, 3527 (2000).
[26] J. E. Hesser et al., Ap. J. **276**, 491 (1984).
[27] G. Cavallo, Astron. Astrophys. **65**, 415 (1978).
[28] J. P. Racchen and P. L. Biermann, Astron. Astrophy. **272**, 161 (1993).
[29] G. R. Farrar, Phys. Rev. Lett. **76**, 4111 (1996).
[30] L. Gonzales-Mestres, *AIP Conf. Proc.* **433**, eds., J. F. Krizmanic et al., 148 (1998).
[31] S. Coleman and S. L. Glashow, Phys. Rev. **D59**, 116008 (1999).
[32] F. A. Aharonian, P. Bhattacharjee, and D. N. Schramm, Phys. Rev. **D 46**, 4188 (1992).
[33] M. Takeda et al., Phys. Rev. Lett. **81**, 1163 (1998).
[34] J. W. Cronin, "Design Concept" memo, Enrico Fermi Institute 92-08 (1992).
[35] J. W. Cronin, Nucl. Phys. **25B** (Proc. Suppl), 61 (1992).
[36] Pierre Auger Design Report, printed by Fermilab (Second edition, November 1996); available electronically at www.auger.org/admin/DesignReport/index.html
[37] P. Sommers, Astropart. Phys. **3**, 349 (1995).
[38] B. R. Dawson et al., Astropart. Phys. **5**, 239 (1996).

[39] M. S. Briggs et al., Ap. J. **459**, 40 (1996).
[40] M. Tegmark et al., Ap. J. **468**, 214 (1996).
[41] T. Stanev et al., Phys. Rev. Lett. **75**, 3056 (1995).
[42] T. Stanev and A. M. Hillas, *Proc. Int. Cosmic Ray Conf.* **4**, 365 (Salt Lake City, 1999).
[43] F. A. Aharonian and J. W. Cronin, Phys. Rev. **D50**, 1892 (1994).
[44] P. Billoir, "Neutrino Capabilities of the Auger Detector," *Proceedings of the 8th International Workshop on Neutrino Telescopes*, ed., M. B. Ceolin (Venice, Papergraf, 1999)
[45] T. K. Gaisser et al., Phys. Rev. **D47**, 1919 (1993).
[46] L. K. Ding et al., Ap. J. **474**, 490 (1997).
[47] Auger technical notes (GAP papers) at www.auger.org under "Technical Info."